

Hydrological Variability and Trends in Global Reanalyses

Junye Chen^(1,2) and Michael G. Bosilovich⁽²⁾

¹ESSIC, University of Maryland; ²GMAO, GSFC NASA

1 INTRODUCTION

A reanalysis is an integration of historical observations and model simulations using data assimilation techniques. Ideally, a long term reanalysis should provide an accurate and comprehensive reconstruction of the history of the climate change. But because of changes of the observation systems and the possible biases in the model and observations, the long term climate variation in the reanalysis data could be contaminated by artificial signals.

In this study, the long term variations in the hydrological fields from the existing reanalyses and independent observations are investigated and intercompared. It is found that the hydrological trends can be very different in different datasets. These differences can be attributed to the different model/observation biases and the different assimilated observational data. The hydrological trends based on more recent reanalyses in which more moisture data are assimilated are not necessarily more accurate than those derived from earlier reanalyses with less moisture data assimilated, because of the changes of observation systems and no moisture conservation constraint in the reanalysis system. The consequent energy budgets and large-scale circulation variations are also addressed.

2 DATA SETS

2.1 Global precipitation observation

The Global Precipitation Climatology Project (GPCP) version 2 monthly precipitation analysis (Huffman et al., 1997; Adler, et al., 2003) and the CPC Merged Analysis of Precipitation (CMAP) (Xie and Arkin 1997) datasets are used in this paper as the baseline to compare with the precipitation data from reanalyses. GPCP and CMAP are both merged datasets based on rain gauge observations and satellite retrievals. They are not identical because difference in the input data and merge methods. The difference between

these two datasets can be used as a rough measurement of the uncertainty of global long term precipitation observation.

2.2 Long term global reanalyses

Precipitation, evaporation and column integrated precipitable water from four published global long term reanalyses are analyzed in this paper. The four reanalyses are NCEP/NCAR Reanalysis 1 (kalnay et al., 1996), NCEP-DOE AMIP-II Reanalysis (Kanamitsu et al., 2002), ECMWF 40 Year Re-analysis (ERA-40) (Uppala et al, 2005) and Japanese 25-year Reanalysis (JRA-25).

3 ANALYSIS

3.1 Precipitation climatology

The spatial distribution of long term (1982-2000) precipitation means are shown in Figure 1. All 6 datasets give a similar global pattern: the strong precipitation ($> 7\text{mm/day}$) is located at west Pacific warm pool, south America Amazon, central Africa, along ITCZ, SPCZ and extratropical storm tracks, and subtropics and polar regions are the driest regions on the earth. Except above similarities, in general, the reanalyses are wetter than GPCP and CMAP, especially in the tropical regions. Among the four reanalysis, ERA-40 shows the highest precipitation in the tropics, JRA-25 and NCEP/DOE are next, and NCEP/NCAR has the smallest value which is near the value of GPCP and CMAP. But the pattern of NCEP/NCAR is not as sharp as those in GPCP and CMAP. Above characters are also shown in the zonal mean seasonal cycle plots in Figure 2.

More differences are shown in the maps of the standard deviations of anomalies from climatology annual cycle (Figure 3) than in the maps of long term mean (Figure 1). The diversification shown in Figure 3 implies more discrepancies among the datasets in the interannual or longer time scales, which are not shown in the long term mean plots (Figure 1).

^{*}Corresponding Author Address: Junye Chen, Global Modeling and Assimilation Office, NASA GSFC Code 610.1, Greenbelt, MD 20771 email: jchen@gmao.gsfc.nasa.gov

3.2 The hydrological long term variabilities

The global mean time series of precipitable water (Figure 4), precipitation (Figure 5), evaporation (Figure 6) and P-E (Figure 7) give a simple description about the time evolution of the global hydrological cycle in the four reanalyses.

The differences in precipitable water (Figure 4) among the reanalyses are around or less than 1.5 Kg/m^2 , which is about 6% of the global mean value ($\sim 25 \text{ Kg/m}^2$), and half of the seasonal cycle range ($\sim 3 \text{ Kg/m}^2$). This uncertainty is near to the uncertainty of modern water vapor observation. And there is a 1.5 Kg/m^2 upward shifting in ERA-40 data in early 1970s, coincident with the introduction of satellite data in ERA-40.

The observed precipitation time series from GPCP and CMAP data are shown with the precipitation time series from reanalyses. GPCP and CMAP time series are close to each other, especially in late period. The ranges of the annual cycle in the observed time series are much smaller than the ranges in reanalyses. And there is no increasing trend in the observe precipitation. For the reanalyses, the precipitation time series in Figure 5 are more apart from each other than in the precipitable water plot (Figure 4). In the 2000s, the difference between ERA-40 (or NCEP/DOE) and NCEP/NCAR is about 0.5 mm/day, larger than the annual cycle range of the reanalyses precipitation, which is already an exaggeration if comparing to the annual cycle range of GPCP or CMAP. All four reanalyses precipitation show an increasing trend from 1990s, though the NCEP/NCAR trend is much smaller than that of other reanalyses.

JRA-25 has the highest evaporation value (Figure 6, green) in all four reanalyses, and a shift around 1987, when the SSM/I data included. All evaporation time series have an increasing trend, and the trend from NCEP/DOE is strongest.

In the real world, or an ideal reanalysis, the global precipitation should be balanced by the global evaporation. But in Figure 7, it is clear that the P-E is only roughly balanced in NCEP/NCAR and NCEP/DOE, but severely unbalanced in ERA-40 and JRA-25. For ERA-40, there is a shift around 1972, and large interannual variations after that. Clearly, this shift and the interannual variations could not be natural signal. Since the reanalysis keeps a fixed model and assimilation system for the whole data period, the artificial change in the time series can only introduced by the change of input observation data: the 1972 shift can be attributed to the introduction of VTPR satellite data, and the large interannual variation is

probably related with the change of satellite data too. For example, the introduction of SSM/I data in 1987, which also has significant impact on the JRA-25 data (Figure 7, green). But why the NCEP/NCAR and NCEP/DOE reanalyses can keep balance between precipitation and evaporation, but not more advanced ERA-40 and JRA-25? The key difference is that satellite observed water vapor channel data are assimilated in ERA-40 and JRA-25, but not in NCEP/NCAR and NCEP/DOE. That is, observed water vapor channel data acts as an external net water vapor sources for ERA-40 and JRA-25, in which the analysis water vapor increment does not vary randomly with zero mean. And in NCEP/NCAR and NCEP/DOE, no external water vapor is added in, and the system makes a moisture balance by itself.

Another question is how to explain the change in precipitable water is relative small (Figure 4), but the change in precipitation is relative large (Figure 5)? A possible reason could be the bias of the model. When the model has a bias in water vapor field, for example, a dry bias, the assimilation system will continue to adjust the water vapor field by adding water vapor into the system based on water vapor observation. And since the model has a dry bias, the system has a tendency to dump "extra" water vapor through precipitation. Even the bias is small, so the change in precipitable water is small, the change in precipitation could be large because the water vapor is added in and dumped out with the frequency of the observation data update. That is, more water vapor data are assimilated, more P-E unbalance could be.

4 DISCUSSION

Except unreal P and P-E, the combination of biased model + moisture assimilation could have profound effect on the whole reanalysis dataset if the observation constrain of the dynamic fields is not complete. Extra precipitation means extra latent heat being released into the system, and driving artificial change in the dynamic field. How the dynamic field will change depends on where the water vapor will be dumped. If the system let the water vapor travel for a distance along with the wind field, for example, from subtropical region to equatorial region, then the release of latent heat probably will cause an artificial acceleration of the general circulation.

Comparing with the negligible trend in GPCP and CMAP data, the precipitation positive trends in the reanalyses data are suspicious too.

ACKNOWLEDGEMENT

GPCP data provided by the Laboratory for Atmospheres, NASA Goddard Space Flight Center, from their web site at: <http://precip.gsfc.nasa.gov/>

CMAP data provided by the NOAA/NWS/CPC, from their web site at http://www.cpc.ncep.noaa.gov/products/global_precip/html/wpage.cmap.html

NCEP/NCAR Reanalysis data provided by the NOAA/OAR/ESRL PSD, Boulder, Colorado, USA, from their Web site at <http://www.cdc.noaa.gov/>

NCEP-DOE_Reanalysis 2 data provided by the NOAA/OAR/ESRL PSD, Boulder, Colorado, USA, from their Web site at <http://www.cdc.noaa.gov/>

ERA-40 data provided by the European Centre for Medium-Range Weather Forecasts, from their web site at <http://www.ecmwf.int/>

JRA-25 data provided by the Japan Meteorological Agency (JMA) at their web site at http://jra.kishou.go.jp/index_en.html

Hagemann, S., Hólm, E., Hoskins, B.J., Isaksen, L., Janssen, P.A.E.M., Jenne, R., McNally, A.P., Mahfouf, J.-F., Morcrette, J.-J., Rayner, N.A., Saunders, R.W., Simon, P., Sterl, A., Trenberth, K.E., Untch, A., Vasiljevic, D., Viterbo, P., and Woollen, J. 2005: The ERA-40 re-analysis. *Quart. J. R. Meteorol. Soc.*, 131, 2961-3012. doi:10.1256/qj.04.176

Huffman, G. J. and co-authors, 1997: The Global Precipitation Climatology Project (GPCP) combined data set. *Bull. Amer. Meteor. Soc.*, 78, 5-20.

Xie P., and P. A. Arkin, 1996: Global precipitation: a 17-year monthly analysis based on gauge observations, satellite estimates, and numerical model outputs. *Bull. Amer. Meteor. Soc.*, 78, 2539-2558.

REFERENCE:

Adler, R.F., G.J. Huffman, A. Chang, R. Ferraro, P. Xie, J. Janowiak, B. Rudolf, U. Schneider, S. Curtis, D. Bolvin, A. Gruber, J. Susskind, and P. Arkin, 2003: The Version 2 Global Precipitation Climatology Project (GPCP) Monthly Precipitation Analysis (1979-Present). *J. Hydrometeorol.*, 4, 1147-1167.

Kalnay et al., The NCEP/NCAR 40-year reanalysis project, *Bull. Amer. Meteor. Soc.*, 77, 437-470, 1996.

NCEP-DOE AMIP-II Reanalysis (R-2): M. Kanamitsu, W. Ebisuzaki, J. Woollen, S-K Yang, J.J. Hnilo, M. Fiorino, and G. L. Potter. 1631-1643, Nov 2002, *Bul. of the Atmos. Met. Soc.*

Uppala, S.M., Källberg, P.W., Simmons, A.J., Andrae, U., da Costa Bechtold, V., Fiorino, M., Gibson, J.K., Haseler, J., Hernandez, A., Kelly, G.A., Li, X., Onogi, K., Saarinen, S., Sokka, N., Allan, R.P., Andersson, E., Arpe, K., Balmaseda, M.A., Beljaars, A.C.M., van de Berg, L., Bidlot, J., Bormann, N., Caires, S., Chevallier, F., Dethof, A., Dragosavac, M., Fisher, M., Fuentes, M.,

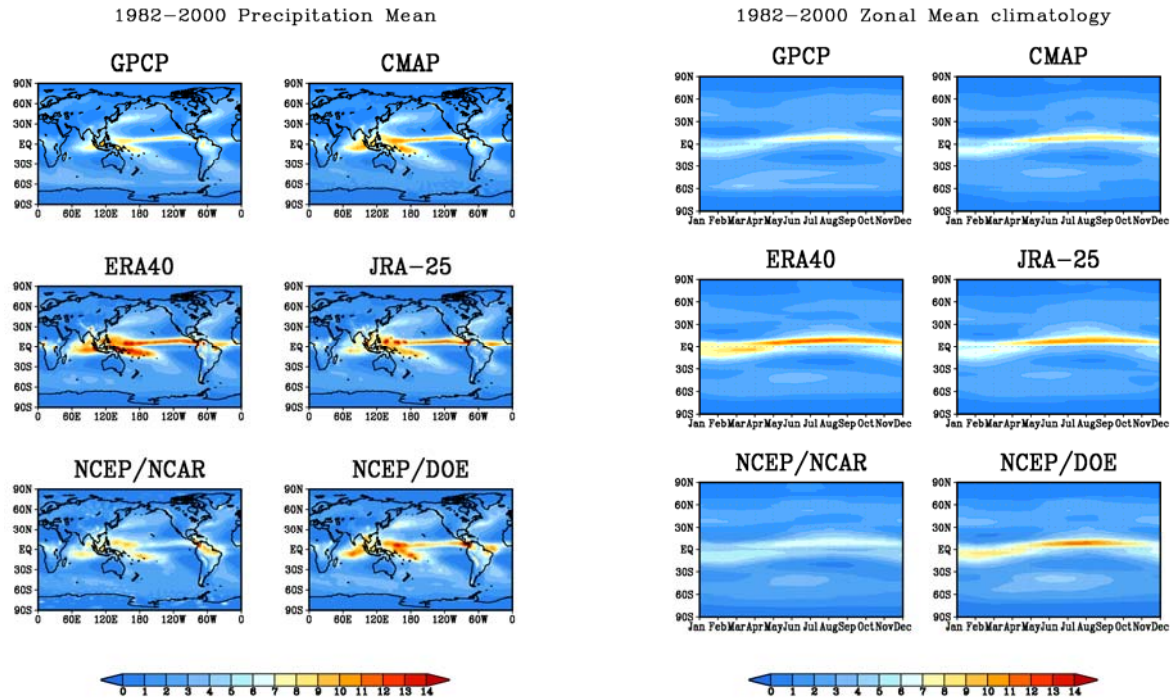


Figure 1. 1982-2000 precipitation mean based on GPCP (top left), CMAP (top right), ERA40 (middle left), JRA-25 (middle right), NCEP/NCAR (bottom left) and NCEP/DOE (bottom right). The unit of color bar is mm/day.

Figure 2. 1982-2000 zonal mean seasonal cycle of precipitation based on GPCP (top left), CMAP (top right), ERA40 (middle left), JRA-25 (middle right), NCEP/NCAR (bottom left) and NCEP/DOE (bottom right). The unit of color bar is mm/day.

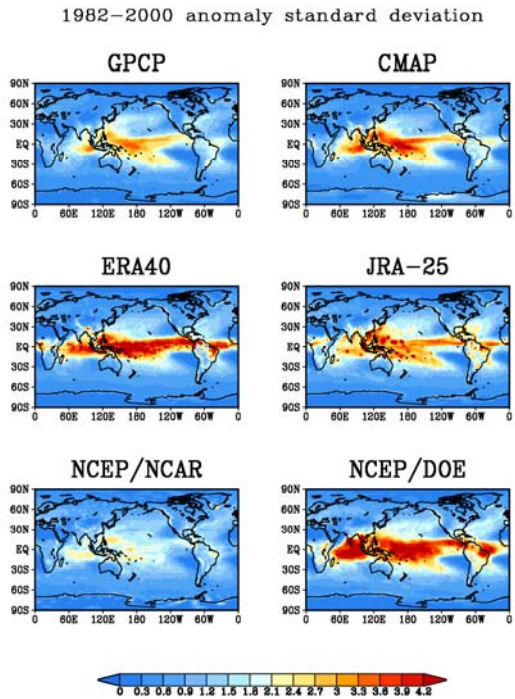


Figure 3. 1982-2000 standard deviation of precipitation anomaly based on GPCP (top left), CMAP (top right), ERA40 (middle left), JRA-25 (middle right), NCEP/NCAR (bottom left) and NCEP/DOE (bottom right). The unit of color bar is mm/day.

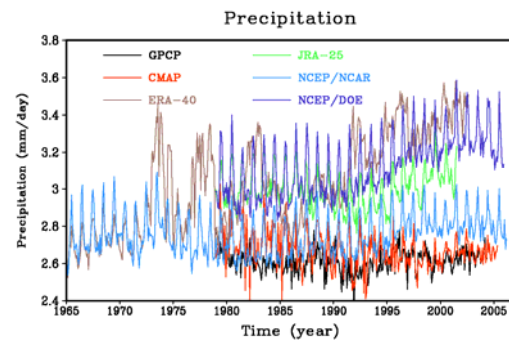


Figure 5. Global mean time series of precipitation based on GPCP (black), CMAP (red), ERA40 (brown), JRA-25 (green), NCEP/NCAR (blue) and NCEP/DOE (purple).

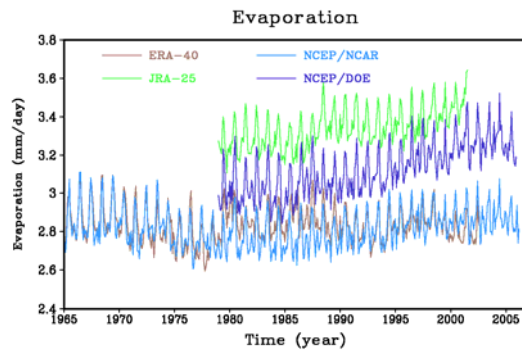


Figure 6. Global mean time series of precipitation based on ERA40 (brown), JRA-25 (green), NCEP/NCAR (blue) and NCEP/DOE (purple).

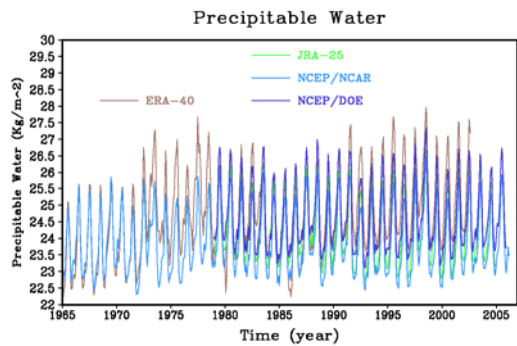


Figure 4. Global mean time series of precipitable water based on ERA40 (brown), JRA-25 (green), NCEP/NCAR (blue) and NCEP/DOE (purple).

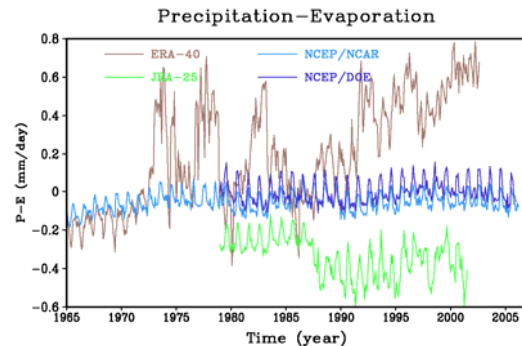


Figure 7. Global mean time series of the difference between precipitation and evaporation based on ERA40 (brown), JRA-25 (green), NCEP/NCAR (blue) and NCEP/DOE (purple).